Electronic structures of GaAs/AlAs lateral superlattices

1998 J. Phys.: Condens. Matter 10 6311

(http://iopscience.iop.org/0953-8984/10/28/012)

J. Phys.: Condens. Matter **10** (1998) 6311–6319. Printed in the UK PII: S0953-8984(98)92280-9

Electronic structures of GaAs/AlAs lateral superlattices

Shu-Shen Li and Bang-Fen Zhu

CCAST (World Laboratory), PO Box 8730, Beijing 100080, People's Republic of China, and National Laboratory for Superlattices and Microstructures, Institute of Semiconductors, Chinese Academy of Sciences, PO Box 912, Beijing 100083, People's Republic of China

Received 6 March 1998, in final form 19 May 1998

Abstract. The electronic energy subbands and minigaps in lateral superlattices (LSLs) have been calculated by the plane-wave expansion method. The effect of the lateral modulation on the critical well width at which an indirect–direct (X–Γ) optical transition occurs in the LSLs is investigated. Our theoretical results are in agreement with the available experimental data. Totally at variance with the previous variation calculational results, the minigaps between the first two subbands in LSLs, as functions of the modulation period, exhibit a maximum value at a specific length and disappear on decreasing the modulation period further. The modulations of several types of lateral potential are also evaluated; the indication is that the out-of-phase modulation on either side of the wells is the strongest while the in-phase modulation is the weakest. Our calculations also show that the effect of the difference between the effective masses of the electrons in the different materials on the subband structures is significant.

1. Introduction

Lateral superlattices (LSLs) are made by imposing a periodic modulation on or in the lateral planes of quantum wells and superlattices. There are two classes of methods of fabricating LSLs. One is constituted by the conventional processing technologies, which produce a direct patterning modulation structure on the surface of the quantum wells by using physical or chemical processing. The smallest modulation period, on the 100 nm scale, has been achieved in the last decade by the use of the processing technologies. The second class of methods of making LSLs is epitaxial growth of periodic structures in the lateral direction. The tilted superlattices and the fractional-layer superlattices, with characteristic lengths of 10 nm or less, belong to this class. Quantum wires may be regarded as the localization limit of the LSLs.

Since the LSLs are ideal systems for which to investigate the effect of dimensionality crossover on the electrical and optical properties of low-dimensional systems, and are useful for exploring the fabrication technology of quantum wires and dots, a great deal of experimental and theoretical research has been carried out on them in the past ten years [1–18]. However, until now, owing the complicated potential pattern on the lateral planes, only a few calculations of the electronic subband structures have been carried out. Sun [15] has recently calculated the minigaps between the first two subbands in GaAs/AlAs LSLs by using a variational calculation based on the simple two-wave approximation—i.e., the trial wave function is composed of products of the ground state of the quantum well and two plane waves in the lateral plane which differ by a reciprocal-lattice vector in the modulation direction. As we shall show, such an approximation is qualitatively acceptable only when the modulation period is much larger than the well width. When the two length scales are

0953-8984/98/286311+09$19.50

comparable or the modulation period is much less than the well width, we shall obtain a quite different variation trend of the minigaps of the LSLs.

It is well known that, in GaAs/AlAs heterostructures, the lowest conduction band state in the constituent GaAs comes from the Γ valley, while that in the constituent AlAs comes from the X valley. If Γ–X mixing can be ignored, two sets of quantized states are formed. The Γ-like levels are mainly confined to GaAs layers and the X-like levels to AlAs layers. For $(GaAs)_l(AlAs)_d$ superlattices, a critical thickness of l_0 can be defined as the well width of the superlattices in which the lowest conduction band state transits from the X-like state to the Γ-like one on increasing l, provided that the barrier width is fixed. For LSLs, however, the effect of the lateral modulation on the Γ–X transition has, to our knowledge, never been reported so far, which is crucial to the optical process in LSLs.

In this paper, we intend to present a simple and efficient calculational model for the electronic subband structure in lateral superlattices, with the emphasis on the effect of modulation on the minigaps of the first two subbands and on the Γ–X transition. Also, we shall evaluate the effect of the differences between the effective masses of GaAs and AlAs on the subband energies in LSLs, which has been shown to be non-negligible for GaAs/AlAs superlattices.

2. The theoretical model

Let l and d be the average GaAs and AlAs widths of the LSLs, respectively; $L_z = l + d$ is the average period of the LSL along the growth direction of the LSLs, which is taken to be the z-direction. The interfaces between the GaAs and AlAs are at $z = nL_z \pm l/2 \pm f_\pm(x)$ ($n = 0, \pm1, \pm2, \ldots$), where $f_\pm(x)$ represent the periodical modulation structures on the lateral planes.

According to Burt and Foreman's effective-mass envelope function theory [20, 21], neglecting the second- and higher-order terms, the effective Hamiltonian of the electrons can be written as follows:

$$H = \boldsymbol{P}\frac{1}{2m^*(\boldsymbol{r})}\boldsymbol{P} + V(\boldsymbol{r}) \tag{1}$$

where $\boldsymbol{P}$ is the electron momentum operator, and

$$m^*(\boldsymbol{r}) = \begin{cases} m_1^* & \text{for } -l/2 - f_-(x) < z - nL_z < l/2 + f_+(x) \\ m_2^* & \text{elsewhere} \end{cases} \tag{2}$$

$$V(\boldsymbol{r}) = \begin{cases} 0 & \text{for } -l/2 - f_-(x) < z - nL_z < l/2 + f_+(x) \\ \Delta V_c & \text{elsewhere.} \end{cases} \tag{3}$$

m_1^* and m_2^* are the electron effective masses in the materials GaAs and AlAs, respectively, which can be anisotropic along different coordinate directions, with components denoted by $m_{1,i}^*$ and $m_{2,i}^*$ ($i = x, y, z$). The electron envelope function equation is

$$H\Psi = E\Psi. \tag{4}$$

To make further calculations, we must specify the periodical interface structure. As a model for the calculation, we assume that

$$f_\pm(x) = \Delta l^\pm \cos\left(\frac{2\pi x}{L_x}\right) \tag{5}$$

where $\Delta l^\pm$ and L_x are the amplitude and period of the modulation structure. Our method can easily be extended to calculate the electronic state in other LSLs with various forms of

potential. When $\Delta l^- = 0$, equation (5) reduces to equation (11) of reference [15]. Clearly, the present model is more general than the model of reference [15].

Using the plane-wave expansion method, we assume that the electron wave functions have the following forms:

$$\Psi(\boldsymbol{r}) = \frac{1}{\sqrt{L_x L_z}} \mathrm{e}^{\mathrm{i}k_y y} \sum_{nm} C_{nm} \exp\{\mathrm{i}\left[(k_x + nK_x)x + (k_z + mK_z)z\right]\} \tag{6}$$

with $K_x = 2\pi/L_x$, $K_z = 2\pi/L_z$, and $n, m = 0, \pm 1, \pm 2, \ldots$. The matrix elements of Hamiltonian (1) for equation (6) can be written as

$$\sum_i \left(\frac{\hbar^2}{2m^*_{1,i}} \delta_{nn'} \delta_{mm'} - \frac{\hbar^2}{2m^*_{12,i}} S_{nm,m'n'} \right) \kappa_i + S_{nm,m'n'} \, \Delta V_c \tag{7}$$

where

$1/m^*_{12,i} = 1/m^*_{1,i} - 1/m^*_{2,i}$ with $i = (x, y, z)$

$\kappa_x = (k_x + nK_x)(k_x + n'K_x)$ $\kappa_y = k_y k_y$ $\kappa_z = (k_z + mK_z)(k_z + m'K_z)$.

$\delta_{nn'}$ is a δ-function:

$$\delta_{nn'} = \begin{cases} 1 & \text{for } n = n' \\ 0 & \text{for } n \neq n'. \end{cases} \tag{8}$$

In equation (7), when $m \neq m'$,

$$S_{nm,m'n'} = \frac{\mathrm{i}}{2\pi(m - m')} (e^+ J^+ - e^- J^-) \tag{9}$$

where

$$e^\pm = \exp\{\pm \mathrm{i}\pi[(m - m')l/L_z + (n - n')/2]\}$$
$$J^\pm = J_{n-n'}[2\pi(m - m')\Delta l^\pm / L_z]$$

and $J_n(x)$ is the nth-order Bessel function of x. When $n = n'$ and $m = m'$,

$$S_{nm,m'n'} = \frac{d}{L_z}. \tag{10}$$

When $n - n' = \pm 1$ and $m = m'$,

$$S_{nm,m'n'} = -\frac{\Delta l^+ + \Delta l^-}{2L_z}. \tag{11}$$

And when $n - n' \neq 0$ or ± 1, and $m = m'$,

$$S_{nm,m'n'} = 0. \tag{12}$$

Thus, the electron subbands in LSLs can be worked out from equation (7).

Table 1. The energy band parameters of bulk GaAs and AlAs used in our calculations.

	Energy gap (eV)		Effective mass (in units of m_0)		
Material	E_g^Γ	E_g^X	m_e^Γ	m_{le}^X	m_{te}^X
GaAs	1.5192	1.981	0.0665	1.9	0.19
AlAs	3.14	2.25	0.15	0.88	0.25

3. Results and discussion

In our calculation, the bulk energy band-structure parameters of GaAs and AlAs are taken from reference [19] as shown in table 1. The conduction band offsets are taken to be 1.06 eV at the Γ point [15] and 0.2918 eV at the X point. The number of plane waves expanded in both the x- and z-directions is 21 in our calculations—namely those with $n, m = 0, \pm 1, \pm 2, \ldots, \pm 10$—and, using these, several of the lowest subbands can be accurately described.

In calculating the X-like states, we neglect the coupling between non-equivalent valleys. Because of the anisotropy in the effective mass in the X valley, three sets of X-like states can be obtained, each taking the longitudinal component of the effective mass in a different spatial direction.

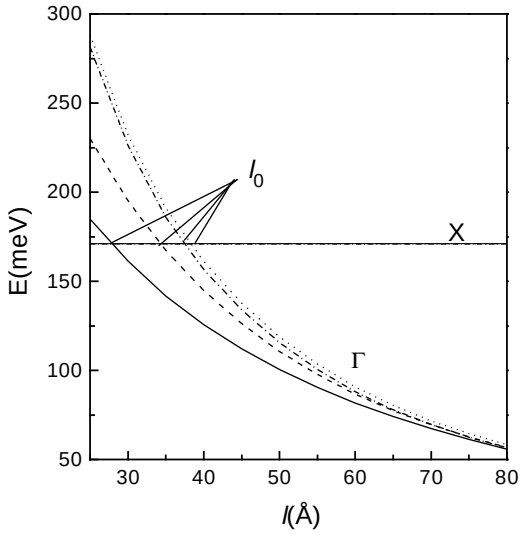

Figure 1. The lowest electron energy levels of X and Γ as functions of the GaAs average thickness l for the AlAs average thickness $d = 200$ Å; $L_x = 200$ Å, $\Delta V_c^{\Gamma} = 1.06$ eV, $\Delta V_c^{\mathrm{X}} = 0.2918$ eV; $\Delta l^+ = \Delta l^- = 10$ Å (solid lines), $\Delta l^+ = -\Delta l^- = 10$ Å (dotted lines), $\Delta l^+ = 10$ Å and $\Delta l^- = 0$ (dashed lines), and $\Delta l^+ = \Delta l^- = 0$ (chain lines), respectively. The effective masses of the electron are taken from table 1.

Figure 1 gives the lowest electron energy levels of X and Γ as functions of the GaAs average thickness l with a fixed AlAs average thickness $d = 200$ Å, and a fixed modulation period $L_x = 200$ Å. The four cases of interfaces studied are $\Delta l^+ = \Delta l^- = 10$ Å (solid lines), $\Delta l^+ = -\Delta l^- = 10$ Å (dotted lines), $\Delta l^+ = 10$ Å and $\Delta l^- = 0$ (dashed lines), and $\Delta l^+ = \Delta l^- = 0$ (chain lines). From our calculations, we have found the following trends.

(i) When the GaAs average thickness is smaller than a critical value l_0, the first Γ-like level of the electron is higher than the X-like level, and a direct-optical-transition LSL is changed to an indirect one.

(ii) The lateral periodical structures can significantly affect the critical value of l_0. l_0 takes its minimum and maximum values when two adjacent faces are out-of-phase ($\Delta l^+ = \Delta l^- = 10$ Å) and in-phase ($\Delta l^+ = -\Delta l^- = 10$ Å) modulations, respectively.

(iii) The critical value of l_0 is strongly dependent on the conduction band offset of the Γ valley at the hetero-interfaces. For larger conduction band offsets, since the X valley in AlAs rises relative to the Γ valley in GaAs, the lowest Γ-like level descends relative to the

lowest X-like level, and the value of l_0 decreases.

(iv) The first Γ-like level of the electron has a lower confinement energy for two faces being out-of-phase modulation or one-face modulation ($\Delta l^+ = 10$ Å and $\Delta l^- = 0$ Å). This is due to the facts that electronic wave functions are more concentrated in the trough zone of the lateral periodical structure, and that the effective well width for the Γ-like electron in these two structures can be considered to be relatively widened. On the other hand, the first subband energy of the Γ-like electron slightly increases under in-phase modulation, reflecting the facts that the motion of the electron along the x-direction is somewhat affected by the lateral periodical structures, and that the effective well width is in fact a little narrowed compared to those for the superlattices without modulation ($\Delta l^+ = \Delta l^- = 0$).

(v) Since the effective masses of the X valley are much larger than those of the Γ valley, the lateral periodical modulation affects the electronic energy little, and the four curves for the X-level energy versus l in the above structures are too close to separate from each other (figure 1).

Table 2. The lowest Γ and X levels of GaAs/AlAs LSLs ($\Delta l^+ = \Delta l^- = 10.2$ Å, $L_x = 32$ Å).

$l = d$ Å	E_Γ (meV)	E_X (meV)
29	304.25	238.61
43	182.06	207.05

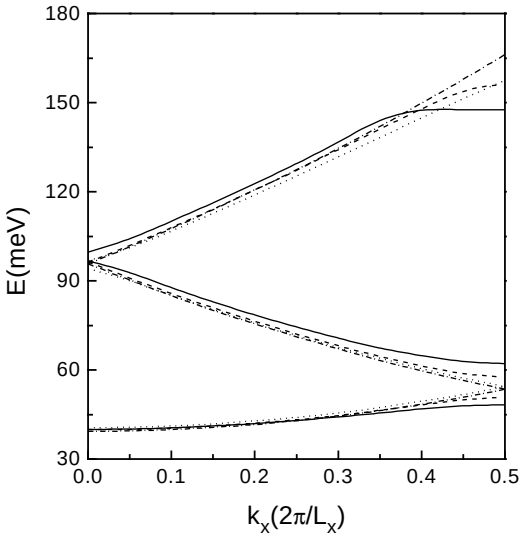

Figure 2. The lowest three subband energy dispersions of Γ electrons as functions of the wavenumber in the x-direction k_x with $l = 100$ Å, $d = 200$ Å, $L_x = 200$ Å, $\Delta V_c^\Gamma = 1.06$ eV, $m^*_{\mathrm{GaAs}} = 0.0665m_0$ and $m^*_{\mathrm{AlAs}} = 0.15m_0$, and with $\Delta l^+ = \Delta l^- = 10$ Å (solid lines), $\Delta l^+ = -\Delta l^- = 10$ Å (dotted lines), $\Delta l^+ = 10$ Å and $\Delta l^- = 0$ (dashed lines), and $\Delta l^+ = \Delta l^- = 0$ (chain lines).

Notzel *et al* reported on the direct synthesis of a superlattice with lateral corrugation of the interfaces on (311) GaAs substrates by molecular beam epitaxy [22]. The structure was shown in the figure 1 of reference [22]. The lateral corrugation can be simplified to a cosine

function with $L_x = 32$ Å and $\Delta l^+ = \Delta l^- = 10.2$ Å. Recently, Jiang *et al* investigated two GaAs/AlAs samples with $l = d = 29$ Å and 43 Å, and found that the 29 Å sample was an indirect-band-gap corrugated superlattice, while the 43 Å one was a direct-band-gap corrugated superlattice [23]. Our theoretical results, as shown in table 2, agree well with the experimental results.

In figure 2, we show the subband energy dispersion relations of the Γ electron as functions of the electronic wavenumber k in the x-direction for samples with $l = 100$ Å, $d = 200$ Å, $L_x = 200$ Å, and with $\Delta l^+ = \Delta l^- = 10$ Å (solid lines), $\Delta l^+ = -\Delta l^- = 10$ Å (dotted lines), $\Delta l^+ = 10$ Å and $\Delta l^- = 0$ (dashed lines), and $\Delta l^+ = \Delta l^- = 0$ (chain lines). From figure 2, we can see that the minigap between the first two subbands depends on the lateral structures in the LSL, which is larger for the out-of-phase and one-side modulation (solid and dashed lines), and small for the in-phase modulation (dotted lines). Thanks to the larger number of plane waves used in these numerical calculations, high-subband-energy dispersions can be accurately obtained, and our data on the minigap between the first and the second subbands are more reliable.

Figure 3(a) shows the minigap ΔE between the first and the second subbands of Γ electrons as a function of the modulation period L_x of the LSLs, where $l = 100$ Å, $d = 200$ Å, and $\Delta l^+ = \Delta l^- = 10$ Å for the solid lines, and $\Delta l^+ = 10$ Å and $\Delta l^- = 0$ for the dotted lines. ΔE tends to be constant when L_x is long enough, which is similar to the result from reference [15], but quite different from that from the two-wave approximation which is that ΔE is a monotonically decaying function of L_x; our calculation shows that, when L_x decreases, ΔE first increases, then reaches a maximum, and finally vanishes just as rapidly. This can be explained as follows. When the modulation period L_x is large compared with l, the reciprocal-lattice vector in the x-direction, K_x, is much smaller than π/l, and thus the state at the bottom of the second subband is just the folded plane wave with K_x perturbed by the modulation. But, when L_x is comparable with l, the folded plane wave may possibly anticross with the plane wave associated with the second confined level in the GaAs/AlAs superlattice without modulation, thus forming the second subband in the LSL. Then, the second subband has two energy minima, one at the point $k_x = 0$ and another at $k_x = 0.5K_x$. When the bottom of the second subband is at the point $k_x = 0$ instead of $0.5K_x$, the minigap decreases upon decreasing L_x, and finally vanishes when the bottom of the second subband is below the top of the first subband. In the simple two-wave approximation, only one subband in the superlattice without modulation evolves, so that an incorrect trend was obtained when L_x was comparable to or less than l.

Figure 3(b) shows ΔE versus the average GaAs thickness l of the LSLs with $L_x = d = 200$ Å, and with $\Delta l^+ = \Delta l^- = 10$ Å (solid lines), and $\Delta l^+ = 10$ Å and $\Delta l^- = 0$ (dotted lines). When l decreases, the modulation effect is enhanced, and ΔE increases. When $l = 20$ Å (solid lines) and $l = 10$ Å (dotted lines), the LSLs become quantum wires.

Figure 3(c) shows ΔE versus the modulation amplitude Δl of the LSLs with $l = 100$ Å, $d = 200$ Å, and with $\Delta l^+ = \Delta l^- = \Delta l$ (solid lines), and $\Delta l^+ = \Delta l$ and $\Delta l^- = 0$ (dotted lines). When Δl increases, ΔE first increases, then reaches a maximum, and finally decreases slightly. As for figure 3(b), when $\Delta l^+ = \Delta l^- = 50$ Å (solid lines), and $\Delta l^+ = 100$ Å and $\Delta l^- = 0$ (dotted lines), this figure gives the results for quantum wires.

Replacing AlAs by $Ga_{1-x}Al_xAs$, we can easily change the band offsets by changing the value of x. The minigap ΔE as a function of the band offset ΔV_c is shown in figure 3(d), where $l = 100$ Å, $d = 200$ Å, and where $\Delta l^+ = \Delta l^- = 10$ Å (solid lines), and $\Delta l^+ = 10$ Å and $\Delta l^- = 0$ (dotted lines). When ΔV_c increases, the modulation effect is enhanced and ΔE increases.

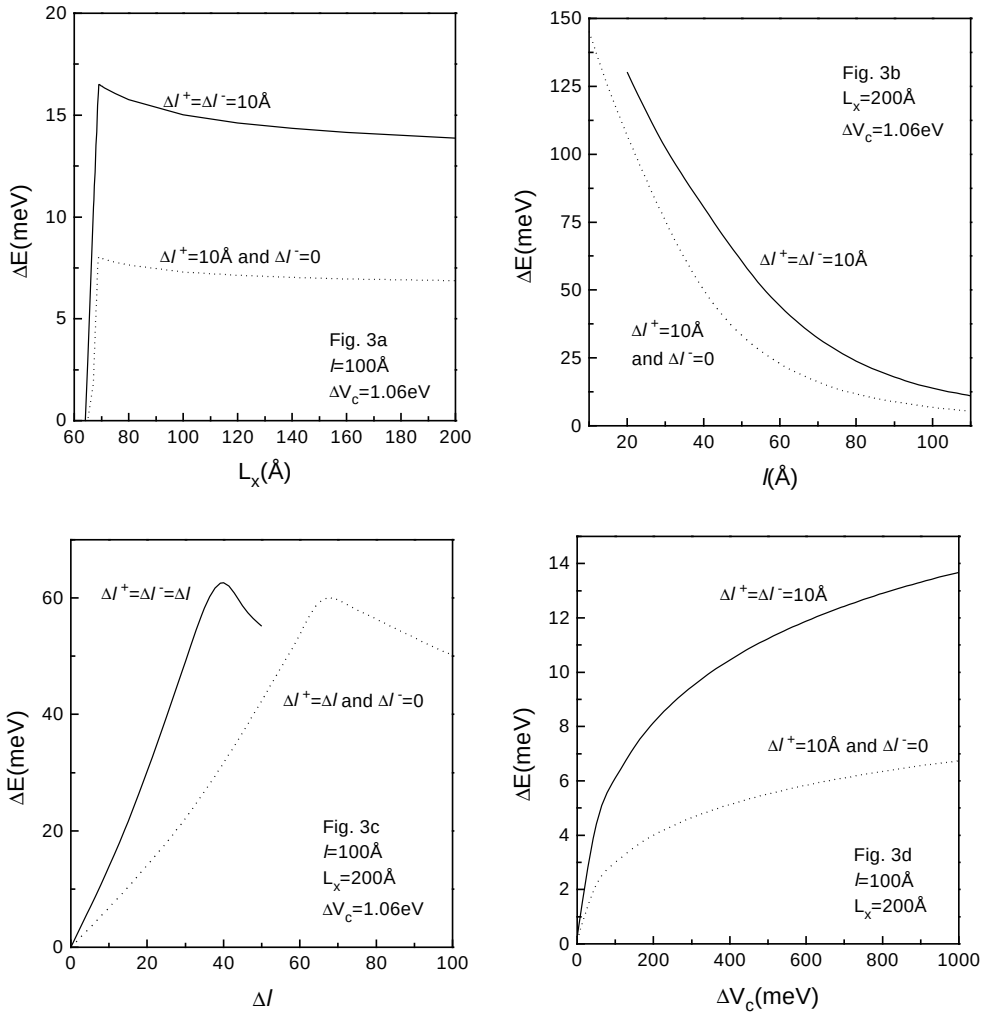

Figure 3. The minigap ΔE between the first and second subband energies of Γ electrons as a function of the modulation period L_x (a), the average well width l (b), the modulation amplitude $\Delta l^{\pm}$ (c), and the band offset ΔV_c^{Γ} (d), with an average barrier thickness $d = 200$ Å, and $m^*_{\mathrm{GaAs}} = 0.0665m_0$ and $m^*_{\mathrm{AlAs}} = 0.15m_0$. The solid lines are for $\Delta l^+ = \Delta l^- \neq 0$, while the dotted lines are for $\Delta l^+ \neq 0$ and $\Delta l^- = 0$

As shown in figure 3, the out-of-phase modulation always leads to larger minigaps than that due to one-side modulation for the same structure parameters. As for the in-phase modulation, close to the case for superlattices without modulation, the minigap almost vanishes, and so this case is not plotted in figures 3(a)–3(d).

To examine the effect of the difference between the effective masses of the electrons in the well and in the barrier materials on the energy subband dispersions, we have calculated the electron subband dispersions as functions of the electronic wavenumber in the x-direction k_x with $l = 100$ Å, $d = 200$ Å, $L_x = 200$ Å, and $\Delta l^+ = \Delta l^- = 10$ Å. These are shown in figure 4. The solid and dotted lines are the results of taking $m^*_{\mathrm{GaAs}} = 0.0665m_0$ and $m^*_{\mathrm{AlAs}} = 0.15m_0$, and taking $m^*_{\mathrm{GaAs}} = m^*_{\mathrm{AlAs}} = 0.0665m_0$, respectively. This figure shows

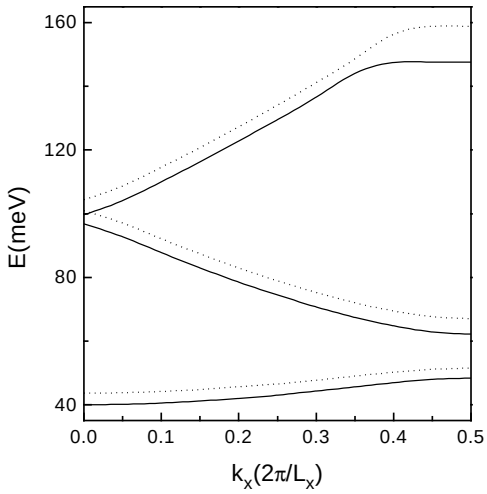

Figure 4. Subband energy dispersions of the Γ electron as functions of the wavenumber in the x-direction k_x, with $l = 100$ Å, $d = 200$ Å, $L_x = 200$ Å, $\Delta V_c^{\Gamma} = 1.06$ eV, and $\Delta l^+ = \Delta l^- = 10$ Å. The solid and dotted lines represent the results obtained when the difference between the effective masses in the well and the barrier are not taken into account, respectively, i.e., $m^*_{\mathrm{GaAs}} = 0.0665m_0$ and $m^*_{\mathrm{AlAs}} = 0.15m_0$ (solid lines), and $m^*_{\mathrm{GaAs}} = m^*_{\mathrm{AlAs}} = 0.0665m_0$ (dotted lines).

that the different effective masses of electrons in different materials significantly affect the subband dispersion, which can be as large as 3.6 meV for the first subband at $k_x = 0$ with the above structure parameters. The difference is even larger than 3.6 meV at other points of the reduced Brillouin minizone in the LSLs.

4. Summary

Within the effective-mass envelope function and plane-wave expansion formalism, the electronic structure for GaAs/AlAs LSLs has been calculated. The effects of the lateral modulation on the energy minigaps between the first and the second subbands and on the critical GaAs layer thickness at which the Γ–X transition occurs in the LSLs have been investigated. Our theoretical results agree well with the available experimental data. Among the three types of modulation studied in this paper, the out-of-phase modulation causes the largest increase of the minigap and decrease of the critical value l_0, while the in-phase modulation has the weakest effect. The minigaps depend strongly on the lateral period when the lateral period is comparable with the well width. Our calculation also indicates the importance of using realistic effective masses of GaAs and AlAs in calculating the subband dispersion.

Acknowledgment

This work was supported by the National Natural Science Foundation of China under Grant No 69736010.

References

[1] Ploog K (ed) 1995 *III–V Quantum System Research (IEE Materials and Devices Series 11)* (Stevenage: IEE) and references therein
[2] Göbel E O and Ploog K 1990 *Prog. Quantum Electron.* **14** 289 and references therein
[3] Brinkop F, Hansen W, Kotthaus J P and Ploog K 1988 *Phys. Rev.* B **37** 6547
[4] Demel T, Heitmann D, Grambow P and Ploog K 1988 *Phys. Rev.* B **38** 12 732
[5] Fukai T and Saito H 1988 *J. Vac. Sci. Technol.* B **6** 1373
[6] Tanaka M and Sakaki H 1988 *Japan. J. Appl. Phys.* **27** L2025
[7] Gerhardts R R, Weiss D and von Klitzing K 1989 *Phys. Rev. Lett.* **62** 1173
[8] Tsuchiya M, Gaines J M, Yan R H, Simes R J, Holtz P O, Coldren L A and Petroff P M 1989 *Phys. Rev. Lett.* **62** 466
[9] Gaines J M, Petroff P M, Kroemer H, Simes R J, Geels R S and English J H 1988 *J. Vac. Sci. Technol.* B **6** 1378
[10] Winkler R W, Kotthaus J P and Ploog K 1989 *Phys. Rev. Lett.* **62** 1177
[11] Kohl M, Heitmann D, Grambow P and Ploog K 1990 *Phys. Rev.* B **42** 2941
[12] Stormer H L, Pfeiffer L N, Baldwin K W, West K W and Spector J 1991 *Appl. Phys. Lett.* **58** 726
[13] Shchukin V A and Efetov K B 1991 *Phys. Rev.* B **43** 14 164
[14] Sham L J 1991 unpublished
[15] Sun H 1992 *Phys. Rev.* B **46** 12 371
[16] Jouanin C, Hallaoui A and Bertho D 1994 *Phys. Rev.* B **50** 1645
[17] Li Shu-Shen and Xia Jian-Bai 1994 *Phys. Rev.* B **50** 8602
[18] Xia Jian-Bai and Li Shu-Shen 1995 *Phys. Rev.* B **51** 17 203
[19] Pavesi L and Guzzi M 1994 *J. Appl. Phys.* **75** 4779
[20] Burt M G 1992 *J. Phys.: Condens. Matter* **4** 6651
[21] Foreman B A 1995 *Phys. Rev.* B **52** 12 241
[22] Notzel R, Ledentsov N N and Ploog K 1993 *Phys. Rev.* B **47** 1299
[23] Jiang D S, Zhou X Q, Oestreich M, Ruhle W W, Notzel R and Ploog K 1994 *Phys. Rev.* B **49** 10 786